WMO GREENHOUSE GAS BULLETIN
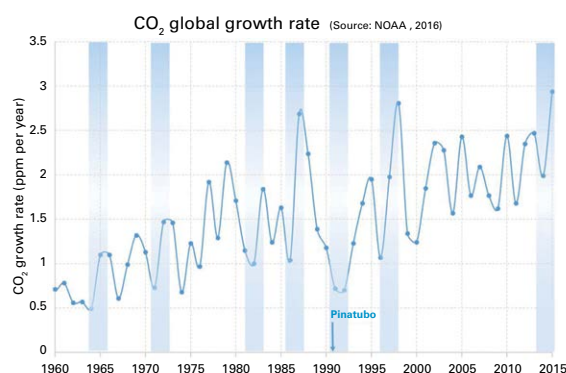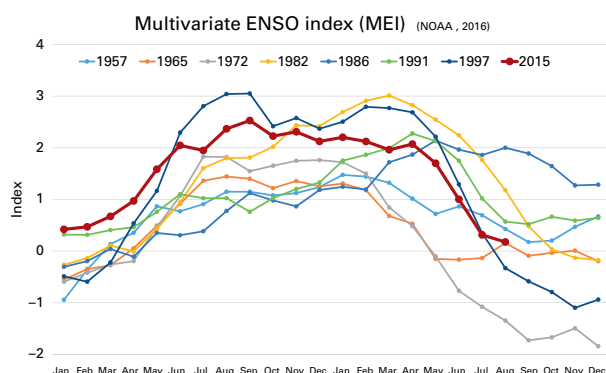
The State of Greenhouse Gases in the Atmosphere Based on Global Observations through 2015

Multivariate ENSO index (MEI) (NOAA, 2016)

CO$_2$ global growth rate (Source: NOAA, 2016)

2015: Changes in greenhouse gases strongly influenced by El Niño

In 2015, Earth experienced the start of a strong El Niño event. El Niño events are natural fluctuations of the climate system where unusually warm water accumulates in the equatorial Pacific Ocean. El Niño events are associated with abnormal weather patterns such as strong storms in some places and droughts or flooding in others. A typical El Niño event lasts 9 months to 2 years. This phenomenon is witnessed roughly every 2–7 years, although such a significant El Niño event had not occurred for the past 18 years.

The figure at left shows the multivariate El Niño/Southern Oscillation (ENSO) index [1] that indicates the strength of the El Niño events. The largest El Niño events since 1950 are shown. The 2015/2016 El Niño was one of the eight strongest since 1950 and was associated with 16 consecutive months of record global temperatures [2]. With the exception of the years following the eruption of Mt Pinatubo in 1991, there has been an increase in the growth rates of atmospheric carbon dioxide (CO$_2$) following El Niño events (figure at right). The plot is based on the CO$_2$ global growth rate as estimated from the National Oceanic and Atmospheric Administration (NOAA) global in situ network [3] with data starting in 1960. The periods with the seven largest El Niño events since 1960 are highlighted in blue.

The CO$_2$ growth rate calculated using observations from the WMO Global Atmosphere Watch (GAW) Programme

is larger than the average of the last 10 years, despite evidence that global anthropogenic emissions remained essentially static between 2014 and 2015. According to the most recent data, increased growth rates have persisted far into 2016, consistent with the expected lag between CO$_2$ growth and the ENSO index. It is predicted that because of this, 2016 will be the first year in which CO$_2$ at the Mauna Loa Observatory remains above 400 ppm[(1)] all year, and hence for many generations [4].

Despite the increasing emissions from fossil fuel energy, ocean and land biosphere still take up about half of the anthropogenic emissions [5]. There is, however, potential that these sinks might become saturated, which will increase the fraction of emitted CO$_2$ that stays in the atmosphere and thus may accelerate the CO$_2$ atmospheric growth rate. During El Niño events, the uptake by land is usually decreased. As during the previous significant El Niño of 1997/1998, the increase in net emissions is likely due to increased drought in tropical regions, leading to less carbon uptake by vegetation and increased CO$_2$ emissions from fires. According to the Global Fire Emissions Database [6], CO$_2$ emissions in equatorial Asia were 0.34 PgC[(2)] in 2015 (average for the period 1997–2015 is 0.15 PgC). Other potential feedback can be expected from changes other than El Niño itself, but rather related to large-scale sea-ice loss in the Arctic, the increase in inland droughts due to warming [7], permafrost melting and changes in the thermohaline ocean circulation of which El Niño is in fact a minor modulator.
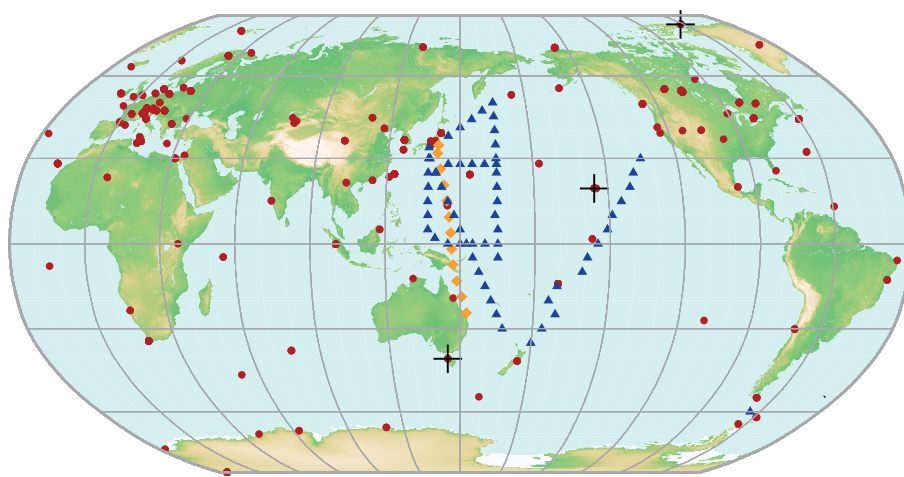
Figure 2. The GAW global network for carbon dioxide in the last decade. The network for methane is similar.
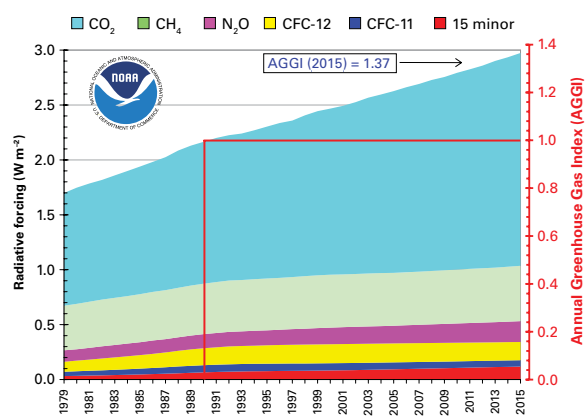

Figure 1. Atmospheric radiative forcing, relative to 1750, of LLGHGs and the 2015 update of the NOAA Annual Greenhouse Gas Index (AGGI) [8, 9]

Table 1. Global annual surface mean abundances (2015) and trends of key greenhouse gases from the WMO/GAW global greenhouse gas monitoring network. Units are dry-air mole fractions, and uncertainties are 68% confidence limits [10]; the averaging method is described in [11].

	CO_2	CH_4	N_2O
Global abundance in 2015	400.0±0.1 ppm	1845±2 ppb	328.0±0.1 ppb
2015 abundance relative to year 1750[a]	144%	256%	121%
2014–2015 absolute increase	2.3 ppm	11 ppb	1.0 ppb
2014–2015 relative increase	0.58%	0.60%	0.31%
Mean annual absolute increase during last 10 years	2.08 ppm yr^{-1}	6.0 ppb yr^{-1}	0.89 ppb yr^{-1}

[a] Assuming a pre-industrial mole fraction of 278 ppm for CO_2, 722 ppb for CH_4 and 270 ppb for N_2O. Stations used for the analyses numbered 125 for CO_2, 123 for CH_4 and 33 for N_2O.
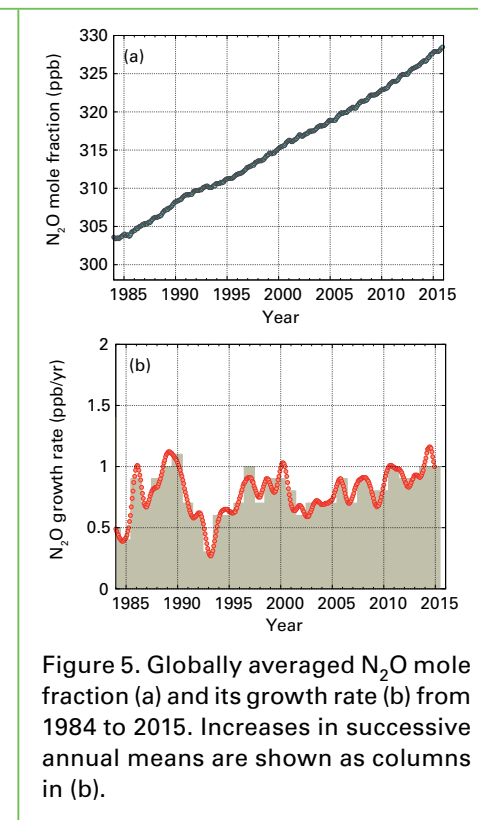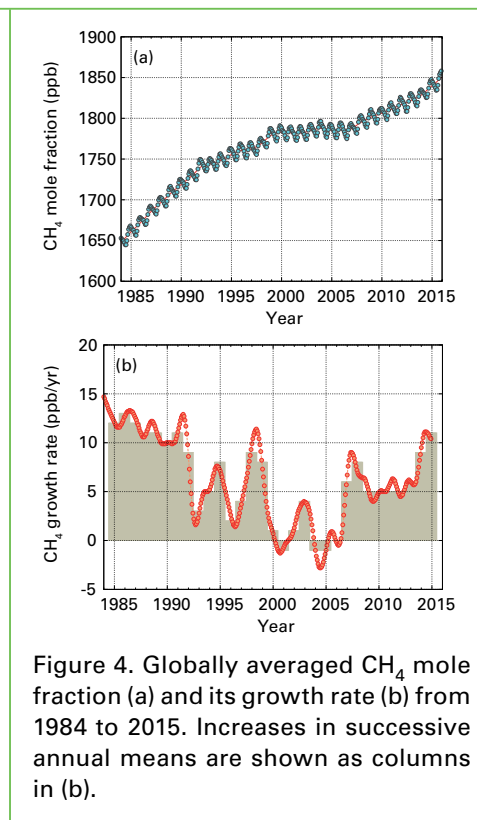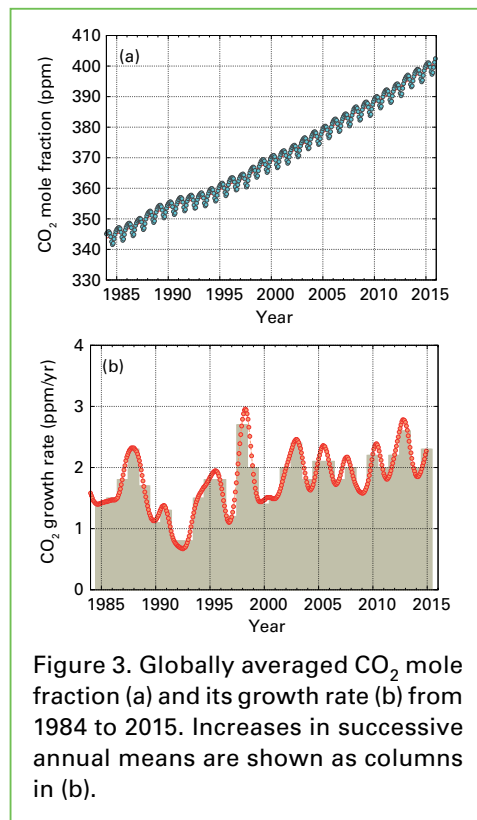
Executive summary

The latest analysis of observations from the WMO Global Atmosphere Watch (GAW) Programme shows that globally averaged surface mole fractions[3] calculated from this in situ network for carbon dioxide (CO_2), methane (CH_4) and nitrous oxide (N_2O) reached new highs in 2015, with CO_2 at 400.0±0.1 ppm, CH_4 at 1845±2 ppb[4] and N_2O at 328.0±0.1 ppb. These values constitute, respectively, 144%, 256% and 121% of pre-industrial (before 1750) levels. It is predicted that 2016 will be the first year in which CO_2 at the Mauna Loa Observatory remains above 400 ppm all year, and hence for many generations [4]. The increase of CO_2 from 2014 to 2015 was larger than that observed from 2013 to 2014 and that averaged over the past 10 years. The El Niño event in 2015 contributed to the increased growth rate through complex two-way interactions between climate change and the carbon cycle. The increase of CH_4 from 2014 to 2015 was larger than that observed from 2013 to 2014 and that averaged over the last decade. The increase of N_2O from 2014 to 2015 was similar to that observed from 2013 to 2014 and greater than the average growth rate over the past 10 years. The National Oceanic and Atmospheric Administration (NOAA) Annual Greenhouse Gas Index [8, 9] shows that from 1990 to 2015 radiative forcing by long-lived greenhouse gases (LLGHGs) increased by 37%, with CO_2 accounting for about 80% of this increase.

Introduction

Since pre-industrial times (before 1750), atmospheric abundances of LLGHGs have risen considerably due to emissions related to human activity. Growing population, intensified agricultural practices, increase in land use and deforestation, industrialization and associated energy use from fossil sources have all led to the increased growth rate of LLGHG abundances in recent years.

It is extremely likely that these increases have led to the global warming that the world is now experiencing [5]. It is also likely that the Earth system will respond to climate change with feedback, including changes in the magnitude of natural fluxes of greenhouse gases. This feedback can increase or decrease the atmospheric growth rate of these

Figure 3. Globally averaged CO₂ mole
fraction (a) and its growth rate (b) from
1984 to 2015. Increases in successive
annual means are shown as columns
in (b).

Figure 4. Globally averaged CH₄ mole
fraction (a) and its growth rate (b) from
1984 to 2015. Increases in successive
annual means are shown as columns
in (b).

Figure 5. Globally averaged N₂O mole
fraction (a) and its growth rate (b) from
1984 to 2015. Increases in successive
annual means are shown as columns
in (b).

gases and thus accelerate or de-accelerate the rate of climate change. The direction and magnitude of this feedback is quite uncertain, but a number of very recent studies hint at a strong influence of future climate change on drought, resulting in weakening of the land sink, further amplifying atmospheric growth of CO_2; that business-as-usual emissions will lead to stronger warming than previously thought; and that melting of Antarctica might lead to twice the maximum sea-level rise thought possible in the last Intergovernmental Panel on Climate Change (IPCC) report, even when the action agreed by the Conference of the Parties to the United Nations Framework Convention on Climate Change (UNFCCC) at its twenty-first session (COP 21) to limit global temperature increase at 2 °C will be reached [12, 13, 14].

Only closely observing the atmosphere with long-term, high-accuracy measurements such as those in the GAW in situ programme, supplemented by satellite observations and numeric modelling, will allow for an understanding of how global atmospheric composition is changing. These observations will also inform as to whether the reduced emissions arising from the COP 21 agreement have the desired effect on atmospheric LLGHG abundances, and whether success will be achieved in reducing these abundances in the long run. This information will guide political decisions on whether even greater mitigation efforts are needed because of the effects of the Earth system feedback mechanisms.

Overview of the GAW in situ network observations for 2015

This twelfth WMO/GAW Annual GHG Bulletin reports atmospheric abundances and rates of change of the most important LLGHGs – carbon dioxide, methane and nitrous oxide – and provides a summary of the contributions of the other gases. These three, together with CFC-12 and CFC-11,

account for approximately 96%[5] [15] of radiative forcing due to LLGHGs (Figure 1).

The WMO Global Atmosphere Watch Programme (http://www.wmo.int/gaw) coordinates systematic observations and analysis of LLGHGs and other trace species. Sites where greenhouse gases are measured in the last decade are shown in Figure 2. Measurement data are reported by participating countries and archived and distributed by the World Data Centre for Greenhouse Gases (WDCGG) at the Japan Meteorological Agency.

The results reported here by WMO WDCGG for the global average and growth rate are slightly different from the results that NOAA reports for the same years [3] due to differences in the stations used, differences in the averaging procedure and the time period for which the numbers are representative. WMO WDCGG follows the procedure described in WMO/TD-No. 1473 [11].

Table 1 provides globally averaged atmospheric abundances of the three major LLGHGs in 2015 and changes in their abundances since 2014 and 1750. Data from mobile stations, with the exception of NOAA sampling in the Pacific (blue triangles in Figure 2), are not used for this global analysis.

The three LLGHGs shown in Table 1 are closely linked to anthropogenic activities and they also interact strongly with the biosphere and the oceans. Predicting the evolution of the atmospheric content of LLGHGs requires quantitative understanding of their many sources, sinks and chemical transformations in the atmosphere. Observations from GAW provide invaluable constraints on the budgets of these and other LLGHGs, and they are used to support the improvement of emission inventories and to evaluate satellite retrievals of LLGHG column averages.

THE INTEGRATED GLOBAL GREENHOUSE GAS INFORMATION SYSTEM

In December 2015, the United Nations Framework Convention on Climate Change adopted the Paris Agreement, codifying the idea of nationally determined contributions (NDCs). The NDCs vary by nation, geographical region and economic ability. Regardless of the strategies and measures applied, the ability to implement long-term policies and manage them effectively will require consistent, reliable and timely information on the magnitude of greenhouse gas (GHG) emissions and their trends over time.

In 2010, the atmospheric, carbon cycle and climate change science communities produced a number of studies [16, 17, 18] on the potential for atmospheric GHG concentration measurements and model analyses to independently evaluate the accuracy of GHG emission inventories produced according to the statistical methods outlined in the 2006 Guidelines of the IPCC Task Force on National Greenhouse Gas Inventories (IPCC TFI) [19]. These reports concluded that a full realization of this approach required additional investment in research, increased density of well-calibrated atmospheric GHG measurements and improved atmospheric transport modelling and data assimilation capabilities.

In recognition of the progress that has been made on the research, measurement and modelling front since 2010, WMO has initiated the development of an Integrated Global Greenhouse Gas Information System (IG3IS) [20]. WMO GAW provides the standards for atmospheric measurements, and IG3IS will establish, propagate and, over time, improve the methodological standards for how atmospheric transport inverse model analyses of atmospheric GHG concentration measurements ("top-down") can be combined with spatially and temporally explicit socioeconomic emission inventory data ("bottom-up") to better inform and manage emission reduction policies and measures.

The IG3IS will serve as an international coordinating mechanism working with many WMO partners, such as the United Nations Environment Programme, the International Bureau of Weights and Measures and the Group on Earth Observations. For the IG3IS initiative to succeed, it must work hard to connect with customers and end users of its information to understand their needs, earn their trust and demonstrate the value of the information they will receive, with the goal of increasingly effective emission-reduction actions. Over time, the IG3IS framework must be capable of promoting and accepting advancing technical capabilities (for example, new satellite observations and sensors), continually improving the quality of and confidence in such information.

The implementation of IG3IS is now under way according to a set of principles and three objective areas defined in the Concept Paper [20]: (1) reduce uncertainty of national emission inventory reporting to UNFCCC; (2) locate, quantify and inform emitters of previously unknown emission reduction opportunities; and (3) provide national and sub-national entities with timely and quantified information on the amounts, trends and attribution of their emissions to support progress towards emission reduction goals. Implementation of IG3IS is proceeding along two lines of activity for each objective area: (1) the initiation of near-term pilot projects that advance the capabilities of selected methods and build confidence in the value of the information with stakeholders; and (2) the preparation of systematic plans for each objective area that will guide nations, states, cities and private enterprises on the implementation of these information systems. A growing number of successful demonstrations for each objective area serve as the bedrock for IG3IS implementation. The following selected examples demonstrate the value of IG3IS.

Continuous methane measurements from four sites on the Swiss Plateau and two additional sites were combined with atmospheric transport simulations and an inverse modelling framework in order to deduce the spatial distribution of CH_4 emissions in Switzerland and adjacent countries [21]. The best inverse estimate of total Swiss CH_4 emissions for the observation period March 2013 to February 2014 is 196±18 Gg yr^{-1}.[6] This value is in close agreement with the national total of 206±33 Gg yr^{-1} reported by Switzerland to UNFCCC in 2015 for the years 2012 and 2013. The combination of the bottom-up and top-down approaches largely confirms the estimate of the reported emission totals, with an uncertainty reduction on the reported value from 16% to 9%.

The inversion system was not set up to optimize emissions by category separately but to estimate the spatial distribution of total emissions. However, information from the inversion on the spatial distribution of the emissions provides qualitative insights into the source categories that dominate in a given region. A robust spatial pattern suggests increased emissions estimated for north-eastern Switzerland (see illustration at top of page 5). Possible candidates for these differences are farming practices between this area and the rest of the country, resulting in different per-head emissions from livestock. Other potential anthropogenic and natural sources may contribute to the unexpectedly high emissions from this area. Further observations will be needed to verify and better characterize this source. Both Switzerland and the United Kingdom of Great Britain and Northern Ireland include top-down information as part of their National Reports to UNFCCC [22].

Global atmospheric concentrations of methane are continuing to grow, but the global growth rate's variability and attribution to both natural and anthropogenic sources are not well understood. Past studies reporting divergent estimates of methane emissions from the oil and gas supply chain have
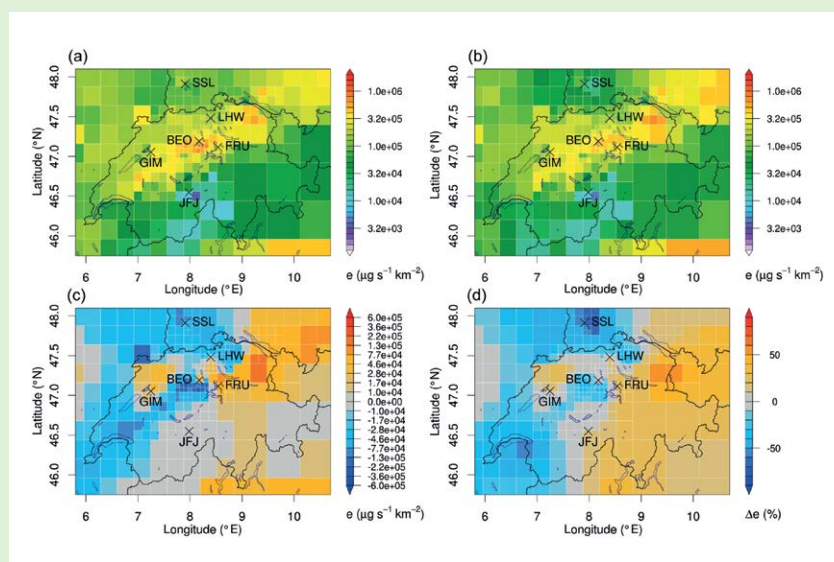
The spatial distribution of the prior emission inventory for Switzerland is shown in (a), posterior emissions are shown in (b), and their absolute and relative difference (posterior minus the prior) are shown in (c) and (d), respectively. An irregular inversion grid was used that exhibits high spatial resolution close to the observation sites (marked by X) and becomes coarser with distance from these sites (source: taken from [21]).
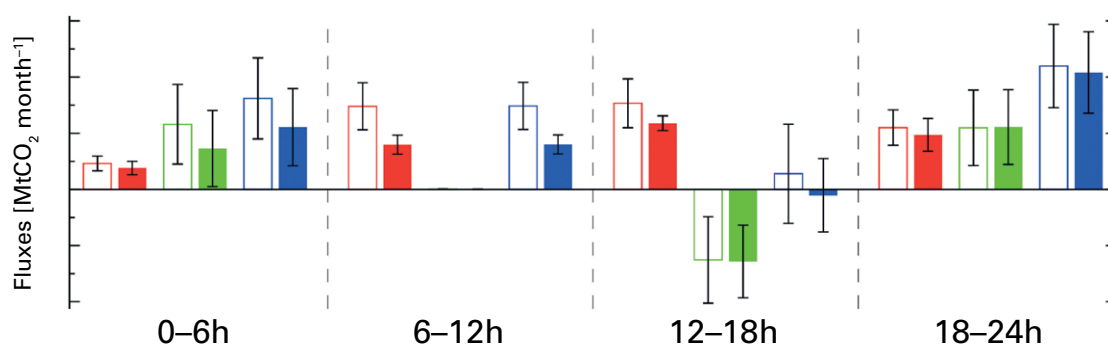
Total flux estimates over a 30-day period, for the four 6-hour periods, for anthropogenic emissions (red), biogenic fluxes (green) and the total (blue). The prior estimates are shown as open rectangles, while the posterior is shown as filled rectangles. Uncertainty reduction is evident for the morning and afternoon time periods (source: taken from [25]).

generated conflicting claims about the full greenhouse gas footprint of this industry. Top-down estimates based on large-scale atmospheric sampling often exceed bottom-up estimates based on source-based emission inventories. Work led by the Environmental Defense Fund and NOAA [23] reconciles top-down and bottom-up methane emission estimates in one of the major natural gas production basins in the United States of America using replicable measurement and data integration techniques. Based on the success of these methods, IG^{3}IS intends to prototype and refine standard methods that can be propagated worldwide and deliver greater confidence and accuracy in characterizing methane emission sources from the oil and gas supply chain. The capability to identify and quantify the small proportion of high-emitting locations will guide oil and gas system operators, as well as methane emissions from waste management and agriculture, to new mitigation opportunities.

The Lima–Paris Action Agenda of the Paris Agreement has formalized a role for sub-national entities such as cities (large urban source regions), which account for more than 70% of

fossil fuel CO_2 emissions. Several studies have shown the potential to better quantify the GHG emissions and trends of cities with atmospheric measurement networks and high-resolution inverse model analyses [24, 25]. The requirements for atmospheric inversion are more demanding in the case of fossil-fuel CO_2 (FFCO$_2$). However, there is evidence that by combining inverse model analysis of a sufficiently dense and well-distributed network of measurements with spatially explicit prior knowledge of sources, urban emissions of FFCO$_2$ can be better quantified [26] (see bottom illustration on this page). While trends in total emissions of FFCO$_2$ from cities are valuable, city planners and managers will need sector-specific information to guide them to emission reduction opportunities. A recent study used an observation system simulation experiment to demonstrate that denser networks of lower-cost, medium-precision measurement sites (30 to 70 for Paris) can produce sector-specific, spatially explicit information on urban emissions [27]. In emerging economies that may have inadequate bottom-up statistical knowledge of emissions from large urban source regions and from natural landscapes, such atmospheric inversion approaches can prove to be especially valuable sources of information.

The NOAA Annual Greenhouse Gas Index (AGGI) [8] in 2015 was 1.37, representing a 37% increase in total radiative forcing (relative to 1750) by all LLGHGs since 1990 and a 1.3% increase from 2014 to 2015 (Figure 1). The total radiative forcing by all LLGHGs in 2015 corresponds to a CO_2-equivalent mole fraction of 485 ppm [9].

Carbon dioxide (CO_2)

Carbon dioxide is the single most important anthropogenic greenhouse gas in the atmosphere, contributing ~65%[5] to radiative forcing by LLGHGs. It is responsible for ~81% of the increase in radiative forcing over the past decade and ~82% over the past five years. The pre-industrial level of ~278 ppm represented a balance of fluxes between the atmosphere, the oceans and the land biosphere. Atmospheric CO_2 reached 144% of the pre-industrial level in 2015, primarily because of emissions from combustion of fossil fuels and cement production (the sum of CO_2 emissions was 9.8±0.5 PgC in 2014), deforestation and other land-use change (0.9±0.5 PgC average for 2005–2014 [7]). The average increase in atmospheric CO_2 from 2005 to 2014 corresponds to ~44% of the CO_2 emitted by human activity with the remaining ~56% removed by the oceans and the terrestrial biosphere. The portion of CO_2 emitted by fossil fuel combustion that remains in the atmosphere (airborne fraction) varies interannually due to the high natural variability of CO_2 sinks without a confirmed global trend.

The globally averaged CO_2 mole fraction in 2015 was 400.0±0.1 ppm (Figure 3). The increase in annual means from 2014 to 2015, 2.3 ppm, is larger than the increase from 2013 to 2014 and the average growth rate for the past decade (~2.08 ppm yr^{-1}). The higher growth rate in 2015 compared with the previous years is due to increased natural emissions of CO_2 related to the most recent El Niño event.

Methane (CH_4)

Methane contributes ~17%[5] to radiative forcing by LLGHGs. Approximately 40% of methane is emitted into the atmosphere by natural sources (e.g. wetlands and termites), and about 60% comes from anthropogenic sources (e.g. ruminants, rice agriculture, fossil fuel exploitation, landfills and biomass burning). Atmospheric CH_4 reached 256% of the pre-industrial level (~722 ppb) due to increased emissions from anthropogenic sources. Globally averaged CH_4 mole fraction calculated from in situ observations reached a new high of 1845±2 ppb in 2015, an increase of 11 ppb with respect to the previous year (Figure 4). The mean annual growth rate of CH_4 decreased from ~13 ppb yr^{-1} during the early 1980s to near zero during 1999–2006. Since 2007, atmospheric CH_4 has been increasing again. Studies using GAW CH_4 measurements indicate that increased CH_4 emissions from wetlands in the tropics and from anthropogenic sources at mid-latitudes of the northern hemisphere are likely causes.

Nitrous oxide (N_2O)

Nitrous oxide contributes ~6%[5] to radiative forcing by LLGHGs. It is the third most important individual contributor to the combined forcing. It is emitted into the atmosphere from both natural (about 60%) and anthropogenic sources (approximately 40%), including oceans, soils, biomass burning, fertilizer use and various industrial processes.

The globally averaged N_2O mole fraction in 2015 reached 328.0±0.1 ppb, which is 1.0 ppb above the previous year (Figure 5) and 121% of the pre-industrial level (270 ppb). The annual increase from 2014 to 2015 is greater than the mean growth rate over the past 10 years (0.89 ppb yr^{-1}). The likely causes are an increase in fertilizer use in agriculture and increased release of N_2O from soils due to an excess of atmospheric nitrogen deposition related to air pollution.

Other greenhouse gases

Sulphur hexafluoride (SF_6) is a potent LLGHG. It is produced by the chemical industry, mainly as an electrical insulator in power distribution equipment. Its current mole fraction is about twice the level observed in the mid-1990s (Figure 6 (a)). The stratospheric ozone-depleting chlorofluorocarbons (CFCs), together with minor halogenated gases, contribute ~12%[5] to radiative forcing by LLGHGs. While CFCs and most halons are decreasing, some hydrochlorofluorocarbons (HCFCs) and hydrofluorocarbons (HFCs), which are also potent greenhouse gases, are increasing at relatively rapid rates, although they are still low in abundance (at ppt[7] levels).
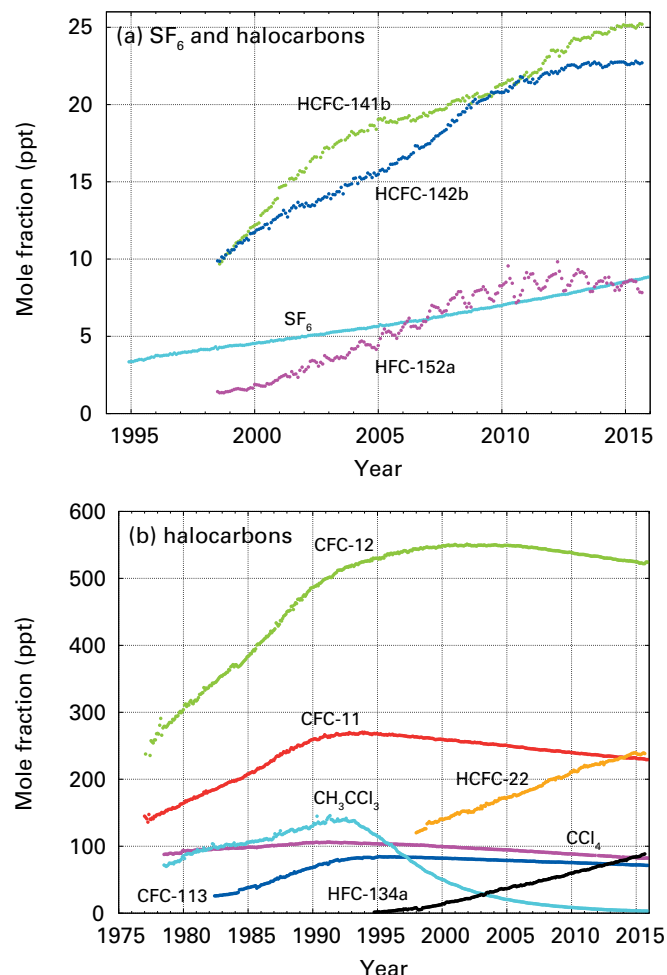

Figure 6. Monthly mean mole fractions of sulphur hexafluoride (SF_6) and the most important halocarbons: SF_6 and lower mole fractions of halocarbons (a) and higher ones of halocarbons (b). The numbers of stations used for the analyses are as follows: SF_6 (24), CFC-11 (23), CFC-12 (24), CFC-113 (23), CCl_4 (21), CH_3CCl_3 (24), HCFC-141b (10), HCFC-142b (14), HCFC-22 (14), HFC-134a (10), HFC-152a (9).

This bulletin primarily addresses long-lived greenhouse gases. Relatively short-lived tropospheric ozone has a radiative forcing comparable to that of the halocarbons. Many other pollutants, such as carbon monoxide, nitrogen oxides and volatile organic compounds, although not referred to as greenhouse gases, have small direct or indirect effects on radiative forcing. Aerosols (suspended particulate matter) are also short-lived substances that alter the radiation budget. All gases mentioned herein, as well as aerosols, are monitored by the GAW Programme, with support from WMO Member countries and contributing networks.

Acknowledgements and links

References

[1] NOAA ESRL, 2016: Multivariate ENSO Index (MEI), http://www.esrl.noaa.gov/psd/enso/mei/.

[2] NOAA, 2016: August marks ongoing trend of record-breaking heat for the globe, http://www.noaa.gov/news/august-marks-ongoing-trend-of-record-breaking-heat-for-globe.

[3] Dlugokencky, E. and P. Tans, 2016: NOAA/ESRL, http://www.esrl.noaa.gov/gmd/ccgg/trends/.

[4] Betts, R.A. et al, 2016: El Niño and a record CO_2 rise. *Nature Climate Change*, 6(9):806–810, doi:10.1038/nclimate3063.

[5] Stocker, T.F. et al., 2013: Technical Summary. In: *Climate Change 2013: The Physical Science Basis. Contribution of Working Group I to the Fifth Assessment Report of the Intergovernmental Panel on Climate Change* (Stocker, T.F., D. Qin et al., eds.). Cambridge University Press, Cambridge, United Kingdom and New York, NY, United States.

[6] Giglio, L., J.T. Randerson and G.R. van der Werf, 2016: Global Fire Emissions Datbase, www.globalfiredata.org.

[7] Le Quéré, C. et al. 2015: Global carbon budget 2015. *Earth System Science Data,* 7(2):349–396, doi:10.5194/essd-7-349-2015.

[8] Butler, J.H. and S.A. Montzka, 2016: The NOAA Annual Greenhouse Gas Index (AGGI), http://www.esrl.noaa.gov/gmd/aggi/aggi.html.

[9] NOAA ESRL, 2016: NOAA's Annual Greenhouse Gas Index, http://www.esrl.noaa.gov/gmd/aggi/.

[10] Conway, T.J. et al., 1994: Evidence for interannual variability of the carbon cycle from the National Oceanic and Atmospheric Administration/Climate Monitoring and Diagnostics Laboratory global air sampling network. *J. Geophys. Res.*, 99:22831–22855.

[11] WMO, 2009: *Technical Report of Global Analysis Method for Major Greenhouse Gases by the World Data Centre for Greenhouse Gases* (Y. Tsutsumi, K. Mori, et al.). GAW Report No. 184 (WMO/TD-No. 1473). Geneva, 29 pp, https://www.wmo.int/pages/prog/arep/gaw/documents/TD_1473_GAW184_web.pdf.

[12] Berg, A. et al. 2016: Land–atmosphere feedbacks amplify aridity increase over land under global warming. *Nature Climate Change,* 6(9):869–874, doi:10.1038/nclimate3029.

[13] Frölicher, T.L., 2016: Climate Response: Strong warming at high emissions. *Nature Climate Change,* 6(9):823–824. doi:10.1038/nclimate3053.

[14] DeConto R.M. and D. Pollard, 2016: Contribution of Antarctica to past and future sea-level rise. *Nature*, 531:591–597, doi:10.1038/nature17145.

[15] IPCC, 2014: *Climate Change 2014: Synthesis Report. Contribution of Working Groups I, II and III to the Fifth Assessment Report of the Intergovernmental Panel on Climate Change* (Core Writing Team, R.K. Pachauri and L.A. Meyer, eds.). IPCC, Geneva, 151 pp.

[16] National Academy of Science, 2010: V*erifying Greenhouse Gas Emissions: Methods to Support International Climate Agreements*. The National Academies Press, Washington, D.C., doi: 10.17226/12883.

[17] Ciais, P. et al., 2010: *GEO Carbon Strategy*. GEO Secretariat, Geneva/FAO, Rome, 48 pp.

[18] IPCC, 2010: *Expert Meeting on Uncertainty and Validation of Emission Inventories* (H.S. Eggleston, J. Baasansuren, K. Tanabe and N. Srivastava, eds.). Meeting Report of the Expert Meeting on Uncertainty and Validation of Emission Inventories, Utrecht, Netherlands, 23–25 March 2010, Pub. IGES, Japan.

[19] IPCC, 2006: *2006 IPCC Guidelines for National Greenhouse Gas Inventories*, http://www.ipcc-nggip.iges.or.jp/public/2006gl/.

[20] WMO, 2016. Integrated Global Greenhouse Gas Information System (IG[3]IS), http://www.wmo.int/pages/prog/arep/gaw/ghg/IG3IS-info.html.

[21] Henne, S. et al., 2016: Validation of the Swiss methane emission inventory by atmospheric observations and inverse modelling. *Atmos. Chem. Phys.*, 16:3683–3710, www.atmos-chem-phys.net/16/3683/2016/.

[22] http://unfccc.int/national_reports/annex_i_ghg_inventories/national_inventories_submissions/items/9492.php.

[23] Zavala-Araiza et al., 2015: Reconciling divergent estimates of oil and gas methane emissions. *PNAS*, 112(51):15597–15602, www.pnas.org/cgi/doi/10.1073/pnas.1522126112.

[24] Lauvaux, T. et al., 2016: High-resolution atmospheric inversion of urban CO_2 emissions during the dormant season of the Indianapolis Flux Experiment (INFLUX). *J. Geophys. Res. Atmos.*, 121, doi:10.1002/2015JD024473.

[25] McKain, K. et. al, 2015: Methane emissions from natural gas infrastructure and use in the urban region of Boston, Massachusetts. *PNAS*, 112(7):1941–1946, doi: 10.1073/pnas.1416261112.

[26] Bréon, F.M. et al., 2015: An attempt at estimating Paris area CO_2 emissions from atmospheric concentration measurements. *Atmos. Chem. Phys.*, 15:1707–1724, http://www.atmos-chem-phys.net/15/1707/2015/acp-15-1707-2015.html.

[27] Wu, L. et al., 2016: What would dense atmospheric observation networks bring to the quantification of city CO_2 emissions? *Atmos. Chem. Phys.*, 16:7743–7771.http://www.atmos-chem-phys.net/16/7743/2016/acp-16-7743-2016.html.

[28] WMO, 2012: *16th WMO/IAEA Meeting on Carbon Dioxide, Other Greenhouse Gases, and Related Measurement Techniques (GGMT-2011). Wellington, New Zealand, 25–28 October 2011* (G. Brailsford, ed.). GAW Report No. 206. Geneva.

Contacts

World Meteorological Organization
Atmospheric Environment Research Division,
Research Department, Geneva
E-mail: gaw@wmo.int
Website: http://www.wmo.int/gaw

World Data Centre for Greenhouse Gases
Japan Meteorological Agency, Tokyo
E-mail: wdcgg@met.kishou.go.jp
Website: http://ds.data.jma.go.jp/gmd/wdcgg/

[1] ppm = number of molecules of the gas per million (10^6) molecules of dry air

[2] 1 PgC = 1 Petagram (10^{15} gram) of carbon

[3] Mole fraction is the preferred expression for abundance (concentration) of a mixture of gases or fluids. In atmospheric chemistry, it is used to express the concentration as the number of moles of a compound per mole of dry air.

[4] ppb = number of molecules of the gas per billion (10^9) molecules of dry air

[5] This percentage is calculated as the relative contribution of the mentioned gas(es) to the increase in global radiative forcing caused by all long-lived greenhouse gases since 1750.

[6] Gg = Gigagram (10^9 gram)

[7] ppt = number of molecules of the gas per trillion (10^{12}) molecules of dry air

Selected greenhouse gas observatories

The Cape Grim Baseline Air Pollution Station (40.68°S, 144.69°E, 94 m a.s.l.) is a fully operational WMO GAW global station. It sits atop the coastal cliff of the far north-west corner of Tasmania, Australia. The prevailing south-westerly winds have typically traversed over long swathes of the Southern Ocean, having had minimal or no contact with land or anthropogenic sources for long time periods, providing an ideal location for baseline sampling in the mid-latitudes of the southern hemisphere. At other times, wind events from the north (trajectories over the city of Melbourne), or from the south-east (over rural agricultural land) allow for episodic sampling under a range of circumstances. The station is operated by the Bureau of Meteorology (BoM), Australia, guided by a science programme jointly managed by BoM and the Australia Commonwealth Scientific and Industrial Research Organization. Collaborative partners include the Australian Nuclear Science and Technology Organization and the University of Wollongong, as well as several international institutions and measurement programmes. Science programmes include particles and multiphase atmospheric chemistry, spectral and passive radiation, ozone/reactive gases, carbon dioxide and its stable isotopes, non-CO_2 greenhouse gases, air archive and radon. Opened in 1976, the station celebrates 40 years of continuous observations and science excellence in 2016.

The Kosetice Observatory (49.58°N, 15.08°E, 534 m a.s.l.) is operated by the Czech Hydrometeorological Institute. It is located in the sparsely-populated agricultural countryside in the Bohemian-Moravian Highlands. The Observatory was established in 1988 as a station specialized in monitoring and research of environmental quality at the regional level in Czechia. The station is focused on air quality (NO_x, O_3, SO_2, CH_4, CO, VOCs, PAHs, precipitation chemistry), selected aerosol and meteorological measurement, among many others. The Observatory has performed continuous observations of CH_4 since 1996 with a gas chromatography. The station is now part of the European Integrated Carbon Observation System network and measures CO_2 and CH_4 with updated equipment.

JN 161640